IBRACON Structures and Materials Journal
Revista IBRACON de Estruturas e Materiais
ISSN 1983-4195 ismj.org

ORIGINAL ARTICLE

Sulfate attack on geopolymer: effect of the proportion of binder and air-entraining additive

Ataque de sulfato em geopolímero: efeito da proporção do ligante e aditivo incorporador de ar

Neusa Aparecida Munhak Beltrame[a]
Vitor Lorival Kudlanvec Junior[a]
Rafaela Souto[b]
Amanda Venancio Trisotto[a]
João Cláudio Nascimento da Silva[b]
Ronaldo Alves de Medeiros-Junior[c]

[a]Universidade Federal do Paraná – UFPR, Programa de Pós-graduação em Engenharia Civil – PPGEC, Curitiba, PR, Brasil
[b]Universidade Federal do Paraná – UFPR, Graduação em Engenharia Civil, Curitiba, PR, Brasil
[c]Universidade Federal do Paraná – UFPR, Centro de Estudos de Engenharia Civil – CESEC, Programa de Pós-graduação em Engenharia Civil – PPGEC, Curitiba, PR, Brasil

Received 26 March 2024
Revised 07 June 2024
Accepted 31 July 2024

Abstract: This research aimed to evaluate the resistance to sodium and magnesium sulfates of geopolymeric mortars, prepared with different proportions of alkaline activators of silicate and sodium hydroxide (Ma), Na_2O content in relation to metakaolin (MK) and silica modulus (Ms). Additionally, an air-entraining additive was also used in an attempt to mitigate the expansive effects of sulfate attack for 20 weeks. The sulfate resistance properties were evaluated by the change in longitudinal length, mass variation, compressive strength, flexural tensile strength, and microstructure. SEM/EDS analyses suggest the formation of caminite and a change in the structure of the aluminosilicate gel to M-A-S-(H) in mortars exposed to $MgSO_4$, while thenardite was indicated as a harmful product in mortars subjected to Na_2SO_4. The experimental results also showed that the greater amount of Na_2SiO_3 in the geopolymer formulation contributes to a denser structure and lower water absorption rate, but resulted in greater physical deterioration and expansion after immersion in sodium magnesium sulfate. The air-entraining additive did not minimize the tensions generated by the sulfate attack. In mortars synthesized with Na_2O/MK = 15% and Ms = 1.5 (GEO-15-1.5) and Na_2O/MK = 22% and Ms = 1.0 and 1.5 (GEO-22-1.0 and GEO-22-1.5), the compressive strengths were similar to standard samples when immersed in $MgSO_4$, while in the Na_2SO_4 solution the increase in strength was attributed to the temporary refinement of the pores by sulfate crystals.

Keywords: geopolymer, metakaolin, sulfate attack, air-entraining additive.

Resumo: Esta pesquisa teve como objetivo avaliar a resistência aos sulfatos de sódio e magnésio de argamassas geopoliméricas, preparadas com diferentes proporções de ativadores alcalinos de silicato e hidróxido de sódio (Ma), teor de Na_2O em relação ao metacaulim (MK) e módulo de sílica (Ms). Além disso, um aditivo incorporador de ar também foi utilizado na tentativa de mitigar os efeitos expansivos do ataque de sulfato por 20 semanas. As propriedades de resistência aos sulfatos foram avaliadas pela mudança no comprimento longitudinal, variação de massa, resistência à compressão, resistência à tração por flexão e microestrutura. As análises MEV/EDS sugerem a formação de caminita e alteração na estrutura do gel de aluminossilicato para M-A-S-(H) em argamassas expostas aos $MgSO_4$, enquanto a tenardita foi indicada como produto deletério em argamassas submetidas aos Na_2SO_4. Os resultados experimentais também mostraram que a maior quantidade de Na_2SiO_3 na formulação do geopolímero contribui para uma estrutura mais densa e menor taxa de absorção de água, mas resultou em maior deterioração física e expansão após imersão em sulfato de sódio e magnésio. O aditivo incorporador de ar não minimizou as tensões geradas pelo ataque de

Corresponding author: Neusa Aparecida Munhak Beltrame. E-mail: neusamunhakbeltrame@gmail.com
Financial support: None.
Conflict of interest: Nothing to declare.
Data Availability: The data that support the findings of this study are available with the corresponding author, [N.A.M.B.], upon reasonable request.

sulfato. Em argamassas sintetizadas com Na_2O/MK = 15% e Ms = 1,5 (GEO-15-1.5) e Na_2O/MK = 22% e Ms = 1,0 e 1,5 (GEO-22-1.0 e GEO-22-1.5), as resistências à compressão foram semelhantes às amostras padrão quando imersas em $MgSO_4$, enquanto na solução de Na_2SO_4 o aumento na resistência foi atribuído ao refinamento temporário dos poros por cristais de sulfato.

Palavras-chave: geopolímero, metacaulim, ataque de sulfato, aditivo incorporador de ar.

How to cite: N. A. M. Beltrame, V. L. Kudlanvec Junior, R. Souto, A. V. Trisotto, J. C. N. Silva, and R. A. Medeiros-Junior, "Sulfate attack on geopolymer: effect of the proportion of binder and air-entraining additive," *Rev. IBRACON Estrut. Mater.*, vol. 17, no. 1, e17114, 2024, https://doi.org/10.1590/S1983-41952024000100014

1 INTRODUCTION

Geopolymers are materials produced by a reaction between an aluminosilicate precursor material and an activating solution [1]. Materials containing silica and alumina can act as precursors, such as metakaolin [2]–[4], fly ash [5], [6], rice husk ash [4], blast furnace slag [7]–[9], and biomass fly ash [10], [11]. Metakaolin is more chemically active at room temperature than other aluminosilicate materials, such as fly ash [12]. The most common alkaline activators used to dissolve precursor materials are sodium hydroxides and sodium silicates, usually a mixture of these components [13], [14]. Several studies have indicated thegood mechanical performance of metakaolin-based geopolymers activated with a combination of Na_2SiO_3 and NaOH [15]–[17].

Sodium silicate is composed of SiO_2, Na_2O, and H_2O and the silica modulus (Ms = SiO_2/Na_2O) is a parameter used to evaluate the properties of geopolymeric materials [18], as it influences the geopolymerization process and, consequently, the pore network and compressive strength [19]. Excess silicate can weaken the structure and reduce the resistance of geopolymers [20]. Furthermore, the concentration of Na_2O can also affect the mechanical performance of geopolymers. Cho et al. [19] demonstrated that the higher concentration of Na_2O contributes to the increase in compressive strength due to the greater dissolution of Si and Al and the generation of more geopolymer synthesis products. However, excess led to a slower strength development because of the precipitation of gels around the surface of the precursor material particles. The choice of initial aluminosilicate also affects the durability of alkali-activated materials [21].

The ability to resist sulfate attack is a crucial longevity factor for concrete materials in aggressive exposure situations, such as marine environments and saline soils [13], [22], [23]. Sulfate attack is a chemical process that involves SO_4^{2-} ions and cement hydration products and the effects are some of the most important factors in the deterioration of concrete structures [24]. In geopolymers, the sulfate attack mechanism is different depending on the calcium content. In high-calcium alkali-activated systems (alkali-activated cement), sulfate attack is similar to that of OPC due to the similarity of the hydration products [25]. In contrast, the degradation of low-calcium alkali-activated systems (geopolymers) involves the exchange of ions between the solution and the network structure [21]. The exchange of OH^- and SO_4^{2-}dominates the ion exchange process in the sodium sulfate solution, while the exchange of Na^+ and Mg^{2+} occurs in the magnesium sulfate solution [22].

Previous research [25] indicated that the presence of gypsum and ettringite decreased the physical and mechanical properties in concrete mixes with higher calcium content, while in systems with low calcium content, the formation of crystals of sodium sulfate in the pores of the material was observed. The low calcium content allows the sulfate solution to exchange ions with the material's internal matrix, forming a less expansive material [25], compared to gypsum and ettringite formed in systems with higher calcium content.

The degradation of geopolymers due to sodium sulfate attack mainly focuses on the effects of pores and cracks within the matrix [13]. Thenardite is indicated as a new phase within the geopolymer and is considered responsible for structural damage and loss of strength [13]. The growth of thenardite in the pores of the material generates crystallization pressure and results in the deterioration of cement mortars, such as cracks and surface peeling [26], and can result in considerable damage [27].

On the other hand, previous research [28] indicated the formation of $Mg(OH)_2$ or M-A-S-(H) phases during exposure to magnesium sulfates due to the counter-diffusion between Mg^{2+} and Na^+. The compound M-A-S-(H), originated by replacing Na^+ from the N-A-S-(H) geopolymeric network with Mg^{2+} from the $MgSO_4$ solution, is indicated as a low resistance phase in other research [29], [30]. Geopolymers are also subject to deterioration in sulfated environments, although the sulfate resistance of these materials is higher compared to Portland cement composites due to the low CaO content of geopolymers [25].

As the mechanical properties of the geopolymer can be affected by several parameters, such as types of binders, SiO_2/Na_2O ratio, type and concentrations of alkaline activators and curing conditions [19], different geopolymer formulations can alter the microstructure of the material and make them less or more susceptible to sulfate attack.

Furthermore, air-entraining additives have been incorporated into cementitious materials to minimize the expansive effects of sulfate attack and freeze-thaw action, as discussed by Ren et al. [31].

The introduction of an air-entraining agent reduces the density and increases the porosity of geopolymer materials due to micro-air bubbles created in the fresh state [32], which is permanent even after hardening [33]. Although the air intake generates a decrease in compressive strength, tensile strength, flexion, and modulus of elasticity [32], [34], the air-entraining additive promotes a constant void system in the concrete that contributes to increasing the durability of the concrete against freezing/thawing cycles, for example. In the research by Aygörmez et al. [33], it was discovered that geopolymeric samples with air-entraining were more stable after the freeze-thaw effect. The reduction in surface tensions provided by controlled, small, and uniformly distributed air bubbles in the samples favored resistance to freeze/thaw cycles. Improvements in resistance to sulfate attack and freeze/thaw action were also indicated in the research of Ren et al. [31].

In this context, the behavior of metakaolin-based geopolymer mortars exposed to sodium and magnesium sulfates for 20 weeks was studied in this research. The variables of this study included different mixtures varying in silica modulus (Ms), molar ratio between alkaline activators (Ma), sodium content in relation to the precursor material (metakaolin), and air-entraining additive. Therefore, in addition to the different geopolymeric formulations, the study of the effect of voids provided by the air-entraining additive was considered, since the sulfate attack results in expansive phases generally accommodated in the pores of the materials. The consequences of this expansive phenomenon result in stresses that can cause cracks and detachment of the material, facilitating the entry of sulfates or other degrading agents into the internal structure of the concrete [35], [36]. Thus, the effect of the voids produced by the additive incorporated into the air in mitigating the expansion of the mortar is also evaluated in this research.

2 MATERIALS AND EXPERIMENTAL PROGRAM

2.1 Materials

2.1.1 Geopolymeric mortar

Commercial metakaolin powder was used as a precursor material in this research. The structure of metakaolin powder was characterized by an X-ray diffractometer (PANalytical), operating at 45 kV and 40 mA, with CuKα 1.2 radiation, wavelength 1.5418 Å. The samples were placed in a zero-bottom silicon sample holder, pressing frontally with a glass slide. The scanning range and step size were 7-70° 2θ and 0.0167° 2θ, respectively, and the samples were rotated horizontally at 2 s/rev, with a counting time of 24.765 seconds and a total time of 2 hours. The main peaks of the diffractogram show that metakaolin is made up of quartz, illite, kaolinite, and microcline, as shown in Figure 1a. The distribution of powdered metakaolin particles was performed using a laser diffractometer model CILAS 920 and measuring range ranging from 0.30 µm to 400 µm (Figure 1b). The average diameter of metakaolin particles is 24.50 µm and 90% of the grains have a diameter smaller than 55.66 µm.

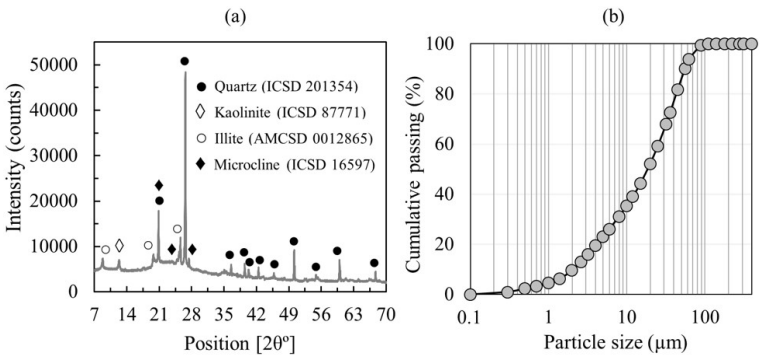

Figure 1. Characterization of metakaolin, (a) XDR, and (b) granulometric distribution.

A combination of sodium hydroxide pearls (97% pure) and sodium silicate, composed of 14.77% Na_2O, 32.26% SiO_2, and 52.97% water, was used to synthesize geopolymeric cement. The water in the sodium silicate solution was

considered in the water/metakaolin ratio. The air-entraining additive used has an alkyl-aryl-sulfonated chemical base and a specific mass between 0.980 and 1.020 g/cm^3. Natural sand with a fineness modulus of 2.01 and a specific density of 2.64 g/cm^3 was used to produce 72 mortar specimens with dimensions of (2.5 × 2.5 × 28.5) cm for variation analysis longitudinal length and mass and 72 mortar specimens with dimensions of (4.0 × 4.0 × 16.0) cm to evaluate the compressive strength and flexural tensile (Table 1).

Table 1. Mixture composition of geopolymer mortars.

Type	MK, g/L	Na_2SiO_3, g/L	NaOH, g/L	W, g/L	Ma	Ms	Na/MK (%)	W/MK, g/g	AE, g/L
GEO-15-1.5	473.3	320.0	30.6	180.7	1.61	1.5	15	0.74	--
GEO-15-1.5-AE	473.3	320.0	30.6	180.7	1.61	1.5	15	0.74	1.89
GEO-22-1.0	465.9	308.0	73.6	181.6	0.65	1.0	22	0.74	--
GEO-22-1.5	463.9	460.0	44.0	99.6	1.61	1.5	22	0.74	--
GEO-22-1.5-AE	463.9	460.0	44.0	99.6	1.61	1.5	22	0.74	1.86
GEO-22-2.0	468.9	620.0	14.9	18.6	6.39	2.0	22	0.74	--

Note: Ma = Na_2SiO_3/NaOH, mol/mol; Ms = SiO_2/Na_2O, mol/mol; Na/MK = sodium/metakaolin; W/MK = water/metakaolin, including water content in Na_2SiO_3; W = additional water; AE = air-entraining additive.

The material ratios of 1:3.2:0.74 (binder:sand:water) were the same for all geopolymer mortar mixtures. The sets of tested specimens and the nomenclature adopted are presented in Table 1. Example: GEO-15-1.5-AE refers to geopolymeric mortar (GEO) with a 15% Na/MK ratio, Na_2SiO_3/NaOH ratio = 1.5 (Ma), and air-entraining additive (AE). GEO-22-2.0 refers to geopolymeric mortar (GEO) with 22% Na/MK ratio and Na_2SiO_3/NaOH ratio = 2.0 (without air-entraining additive), and so on. Furthermore, the acronyms S and M were added to name the samples immersed in the sodium sulfate and magnesium sulfate solution, respectively. The amount of Na_2O was calculated by converting NaOH to Na_2O and the proportion contained in the sodium silicate solution, while the SiO_2 content was the proportion contained in Na_2SiO_3 to determine the molar ratios SiO_2/Na_2O (Ms). The Na/M ratio was determined as a mass percentage of Na_2O in relation to the mass amount of metakaolin.

2.1.2 Geopolymer mixing and curing

Alkaline activators were prepared 24 hours before mixing the mortar. For this, NaOH was dissolved in water and added to Na_2SiO_3. The water used to dissolve the NaOH varied with the amount of Na_2SiO_3 added to the mixture, as shown in Table 1, that is, the amount was obtained from the difference between the total water used in the mortar and the water content contained in the Na_2SiO_3.

The next day, metakaolin was added to the alkaline solution and homogenized in a bench mixer at low speed (140 ± 5 rpm) for 60 s and at high speed (285 ± 10 rpm) for another 30 s to obtain a homogeneous paste. After this time, the speed was reduced and the fine aggregate was added over the next 30 s and mixed at high speed for another 30 s, when the mixer was then turned off for 1 min and 30 s to remove the mortar adhering to the walls of the tank and of the shovel. Immediately after this interval, the mixer was turned on again at high speed for another 60 seconds, resulting in a total mixing time of 5 min (temperature 25 ± 3 °C) and a volume of 0.0052 m^3 per batch of mortar. The mixing procedure was adapted from NBR 13583 [37].

The casting was done in two equal layers with 16 blows in each for consolidation. Then, the prisms were cured in the mold for 24 hours (temperature = 25 ± 3 °C and RH = 50 ± 5%). The specimens were then demolded and stored in a climate chamber at 20 °C and ≈ 95% relative humidity until 84 days of age. As the chemical reactions of Na_2SiO_3 occur more slowly compared to NaOH [38], we chose to extend the curing time, which favors geopolymerization before subjecting the mortars to sulfate attack.

2.1.3 Exposure to sodium and magnesium sulfates

Four mortar specimens were immersed in a solution of sodium sulfate (Na_2SO_4) and magnesium sulfate ($MgSO_4$), with purity greater than 99%. Specimens immersed in deionized water were also tested to calculate the resulting longitudinal length and mass variations. The sodium sulfate mixture ratio was 100 g: 900 g, as recommended by NBR 13583 [37], prepared with deionized water and stored at room temperature for 24 hours. The amount of magnesium sulfate heptahydrate was 173.53 g: 826.47 g. With these proportions, both sodium and magnesium sulfate solutions presented the same amount of sulfate ions (SO_4^{2-}= 67.63 g) per liter of solution. The mortar bars were placed in the solutions with a minimum spacing of 20 mm between the specimens and stored in an oven at a constant temperature of 40 ± 2 °C for 20 weeks.

2.2 Experimental testing

2.2.1 Mass and length change

A digital scale with an accuracy of 0.01 g was used to monitor mass change over time. The mass values of four specimens were recorded and calculated every two weeks until the end of sulfate exposure (week 20). To avoid the effect of the initial saturation degree on the results, the mass variation (Δm) was determined in relation to week 1 of exposure, calculated according to Equation 1. The water absorption rate (ΔAb) was determined, according to Equation 2, during the first week of immersion in water to characterize the permeability of the mortar specimens.

$$\Delta m = \frac{(Mx - Mi)}{Mi}\ x\ 100 \qquad \text{Eq. (1)}$$

Where *Mx* is the mass in week x and *Mi* represents the mass of the specimens after the first week of exposure to sulfates.

$$\Delta Ab = \frac{(Ms - Md)}{Md}\ x\ 100 \qquad \text{Eq. (2)}$$

Where M*s* is the saturated mass and M*d* represents the dry mass before water immersion.

After reading the mass variation, the specimens were placed one by one in the length variation measurement gantry with an accuracy of 0.001 mm, always in the same direction and position. The result of expansion (positive variation) or retraction (negative variation) was calculated (Equation 3) from the difference between the bar reading at age x (Lx) and the bar reading at age 0 (Li), according to NBR 13583 [37].

$$\Delta L = \frac{(Lx - Li)}{Li}\ x\ 100 \qquad \text{Eq. (3)}$$

Where *Lx* is the length in week x and *Li* is the initial length of the specimens before exposure to sulfates.

2.2.2 Compressive and flexural tensile strength

Compressive and tensile strengths were determined at exposure ages of 0 and 20 weeks. The test was carried out in accordance with standard NBR 13279 [39]. A hydraulic press with a loading speed of 10 mm/min was used to break three (tensile strength) and six (compressive strength) specimens for each mixture and exposure condition. Statistical treatment of experimental data was performed using ANOVA analysis of variance and Tukey's test (5% probability of error).

2.2.3 Analyze microstructural

The evaluation of the mortar microstructures was performed by extracting fragments with (2.0 ± 0.5) mm edges and metalized with gold for analysis using scanning electron microscopy (SEM) on a Tescan microscope (model VEGA3 LMU), a voltage of 15 kV and approximation of up to 10 kx. Fragments with the same dimensions were collected and evaluated by energy dispersive X-ray spectroscopy (EDS), Oxford detector, model C-Max 80.

3 RESULTS AND DISCUSSION

3.1 Solution absorption

Figure 2 shows the effect of the geopolymer mortar formulation on water absorption before exposure to sulfate. Table 2 shows the analysis of variance of the data. The addition of air-entrained to the GEO-15-1.5-AE and GEO-22-1.5-AE mixtures (Figure 2a) did not significantly increase the water absorption rate of the samples. Furthermore, it is possible to observe that the higher sodium silicate content (Ms = 1.5 and Ms = 2.0) improved the water absorption of the GEO-22-1.5 and GEO-22-2.0 samples, while the lower sodium/metakaolin content (Na/MK = 15%) produced a structure with lower density compared to samples with Na/MK = 22% (Figure 2b). Previous research has also pointed out that the use of silicates provides a denser microstructure compared to NaOH [20], [40]. Therefore, the geopolymer formulation plays an important role in developing the microstructure and density of the material, which directly affects resistance to sulfate attack. The proportion of voids increases the diffusion of sulfate ions into the samples, which reduces sulfate resistance [12].

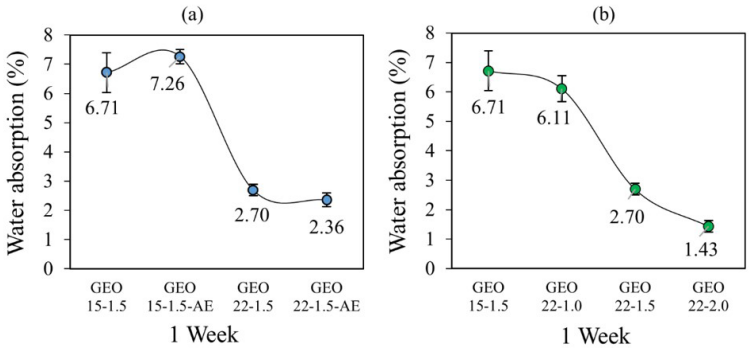

Figure 2. Water absorption by immersion. (a) With air-entraining; (b) No air-entraining.

Table 2. Results of water absorption tests by immersion.

Specimens	Average	S.D.	p-value	Significance level
GEO-15-1.5	6.71	0.67	2.60E-05	Significant
GEO-22-1.5	2.70	0.20		
GEO-22-1.0	6.11	0.44	7.50E-06	Significant
GEO-22-1.5	2.70	0.20		
GEO-22-1.5	2.70	0.20	9.96E-05	Significant
GEO-22-2.0	1.43	0.20		
GEO-15-1.5	6.71	0.67	0.1733	Non-significant
GEO-15-1.5-AE	7.26	0.25		
GEO-22-1.5	2.70	0.20	0.068	Non-significant
GEO-22-1.5-AE	2.36	0.24		

3.2 Visual appearance

Figure 3 shows the visual appearance of the specimens submerged in sodium and magnesium sulfate solutions after 20 weeks of exposure. The most noticeable damage was observed in the sodium sulfate solution when the samples had more sodium silicate as an alkaline activator (GEO-22-2.0-S). The deterioration consisted of cracking of the edges and disintegration of the specimens' surface particles. When immersed in magnesium sulfate solution, a compound was formed on the surface of the GEO-22-2.0-M prisms, but no physical changes occurred during the tests.

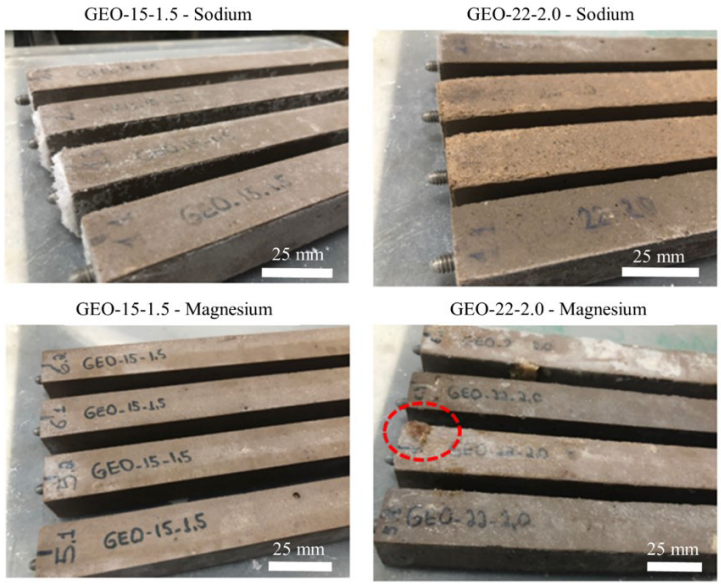

Figure 3. Visual inspection of samples.

SEM/EDS analysis (Figure 4) shows the chemical elements O, Mg, S, and Si, which is a stoichiometric indicator of the formation of caminite ($Mg_3(SO_4)_2(OH)_2$), according to Chen et al. [22]. Caminite was removed from the surface of GEO-22-2.0-M specimens in week 4 and no further compounds were recorded after this period. In the other samples, no physical changes were found throughout the tests.

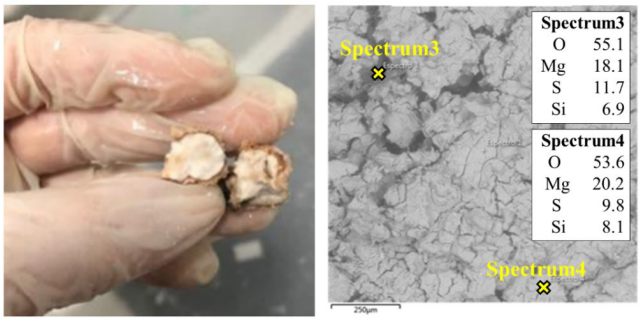

Figure 4. SEM/EDS of the compound formed on the surface of GEO-22-2.0-M after $MgSO_4$ exposure.

3.3 Length and mass change

Figure 5 shows the evolution of the variation in linear length and weight of the specimens submerged in the sodium sulfate solution. According to Figure 5a, all mortar samples showed similar longitudinal variations over the time of exposure to sodium sulfates, except for the GEO-22-2.0-S sample, which showed an expansion close to 0.20%. This expansion generated cracks and disintegration of particles on the surfaces of the specimens, as shown in the visual analysis (Figure 3). Although the longitudinal variation of the GEO-22-2.0-S specimens was greater than the other samples, the low water absorption rate (≈ 1.4%, Figure 2) contributed to the stability of the mass during the tests (Figure 5b).

On the other hand, the lower content of Na/MK = 15% and sodium silicate (Ms = 1.0) used in the mixtures GEO-15-1.5-S and GEO-22-1.0-S increased the mass gain, which is in line with the highest water absorption rates (≈ 6-7%) presented in section 3.1. For the GEO-22-2.0-S samples submerged in the sodium sulfate solution, the peaks of the major chemical elements shown in SEM/EDS spectra 38 and 40 (Figure 6), corresponding to oxygen (O), sulfur (S), and sodium (Na), were attributed to the formation of thenardite (Na_2SO_4) [13], [25], similar to rice grains [26]. Therefore, the expansion and cracks recorded in the GEO-22-2.0-S samples occurred due to the thenardite crystals. The thenardite was also identified in the test specimens of the other mortars. However, the greater porosity compared to the GEO-22-2.0-S samples may have accommodated the sulfate crystals in the pore network, dampening the physical data up to the tested age.

Na_2SiO_3 generally offers higher mechanical resistance to geopolymers than activators with hydroxides [15], [41]. However, it has been previously demonstrated [20] that increasing the amount of this activator can weaken the microstructure. A high concentration of Na_2SiO_3, as in the GEO-22-2.0-S samples used in this research, increased leaching risks due to its high mobility in geopolymers [42]–[44]. Therefore, the expansion of the GEO-22-2.0-S specimens without adding mass suggests the coexistence of alkaline activator leaching and thenardite formation from sulfate attack.

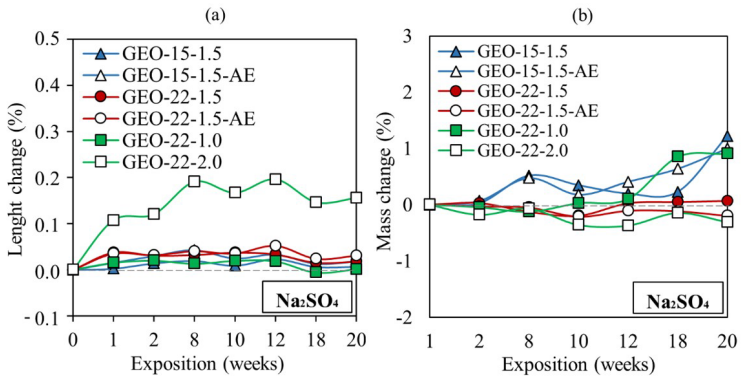

Figure 5. Samples exposed to Na_2SO_4. (a) Change in longitudinal length; (b) Change in mass.

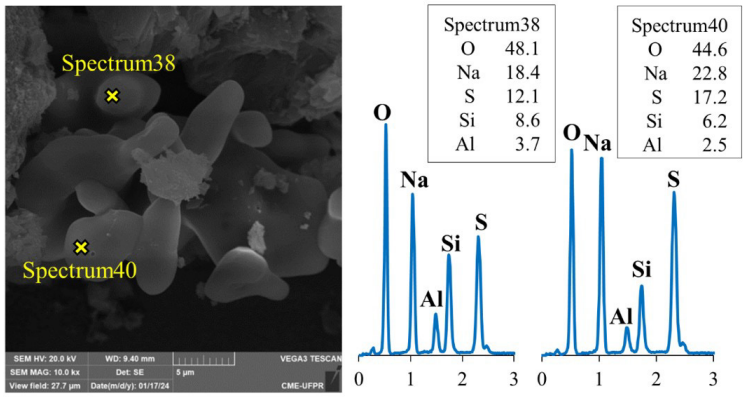

Figure 6. SEM/EDS of GEO-22-2.0-S mortars exposed to sodium sulfate.

According to Figure 5, the voids provided by the air-entraining additive did not influence the longitudinal and mass variation of the mortars exposed to Na_2SO_4, which may be associated with the insufficient time to accumulate the sulfate attack products in the air voids and cause damage to the mortars. Therefore, no benefit of the air-entraining additive was found in this study for the age and conditions tested.

Likewise, the evolution of the variation in the linear length and mass of the specimens submerged in the magnesium sulfate solution is illustrated in Figure 7. Except the GEO-22-2.0-M specimens, all mortars with different formulations showed longitudinal variations of less than 0.10% until the end of the tests (Figure 7a). In the GEO-22-2.0-M specimens, an expansion of around 0.12% was recorded in the first weeks of exposure, but the linear increase in the specimens did not cause surface damage as shown in Figure 3.

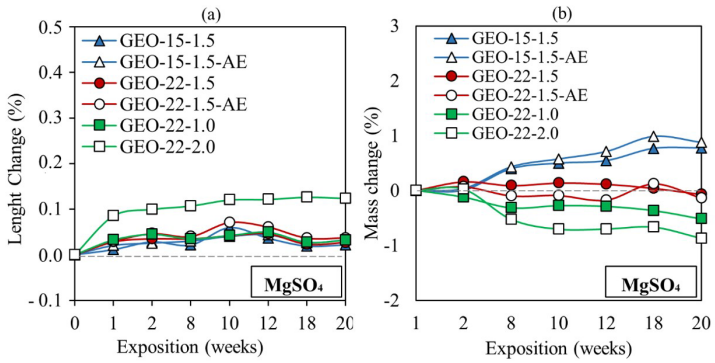

Figure 7. Samples exposed to $MgSO_4$. (a) Change in linear length; (b) Change in mass.

Unlike exposure to Na_2SO_4, the mass of GEO-22-2.0-M reduced slightly due to the removal of caminite originating on the surface of the specimens after four weeks of testing. Furthermore, the absence of mass increase confirms the non-formation of new compounds until the end of the tests. The lower sodium content (Na/MK = 15%) contributes to the increase in mass in samples exposed to magnesium sulfates, and this increase is related to the larger pore network measured by water absorption in the first week of immersion in water (6-7%). Therefore, the larger pore network could increase the diffusion of sulfate ions and, as a consequence, result in greater mass gains, as occurred in mixtures with Na /MK = 15%.

On the other hand, it is possible to notice a reduction in weight in geopolymers formulated with Ms = 1.0 and Ms = 2.0 (GEO-22-1.0-M and GEO-22-2.0-M). It is reported in previous research that Na_2SiO_3 is more susceptible to leaching than NaOH [43], [44], which would align with this research. Therefore, a greater drop in mass could be attributed to the use of the alkaline activator Na_2SiO_3 in mixtures with Ms = 2.0 and the internal decrease in mixtures GEO-22-1.0-M (Ms = 1.0) justified by insufficient geopolymerization [15] and higher permeability shown in Figure 2b (6.11%). According to Phair et al. [45], moderate leaching occurs when a combination of NaOH and Na_2SiO_3 are used together, which justifies maintaining the weight of samples GEO-22-1.5-M and GEO-22-1.5-AE-M throughout the tests. Furthermore, no benefit of the air-entraining additive was found in mortars exposed to magnesium sulfates.

In the $MgSO_4$ solution, spectrum27 (Figure 8) shows the chemical elements corresponding to oxygen (O), silicon (Si), aluminum (Al), and greater amounts of magnesium (Mg), which was attributed by stoichiometric calculations to the formation of the M-A-S-(H), considered to be of low resistance in previous research [28]. Aluminosilicate gel with magnesium sulfate was also reported in Jena and Panigrahi's research [29].

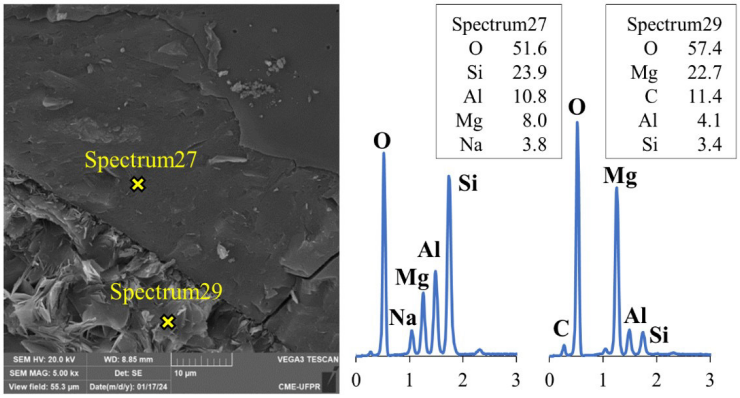

Figure 8. SEM/EDS of GEO-22-1.5-M mortars exposed to magnesium sulfate.

Therefore, the exchange of Na^+ in the geopolymeric networks with Mg^{2+} from the $MgSO_4$ solution occurred, giving rise to a new M-A-S-(H) phase. Furthermore, $MgCO_3$ phases (spectrum29) may have originated during sample preparation due to the difficulty of keeping them without contact with atmospheric air. Crystals resulting from magnesium sulfate attack are larger than sodium sulfate crystals [22]. Furthermore, hydrated magnesium silicate gel (M-S-H) can coexist with N-A-S-(H) aluminosilicate gel and densify the geopolymer matrix.

3.4 Compressive and tensile strength

Figure 9 and Table 3 shows the effect of sodium and magnesium sulfate attack on compressive strength. Although the crystallization of thenardite in the pores is considered harmful to the material due to internal pressure and cracking [26], [27], in this study, a significant gain in compressive strength up to 19.6% was found in most samples immersed in the solution of sodium sulfate. This increase in compressive strength may be associated with temporary pore refinement cycles [46], [47]. According to Luo et al. [48], sulfate enters the samples, causing the deposition of expansive products (sulfate crystals) to fill some pores in the material, densifying the samples and contributing to an increase in compressive strength. As Na_2SO_4 crystals continue to precipitate and deposit in the pores of the sample, stresses increase, resulting in expansion and cracking. Thus, a new cycle is restarted until the material deteriorates.

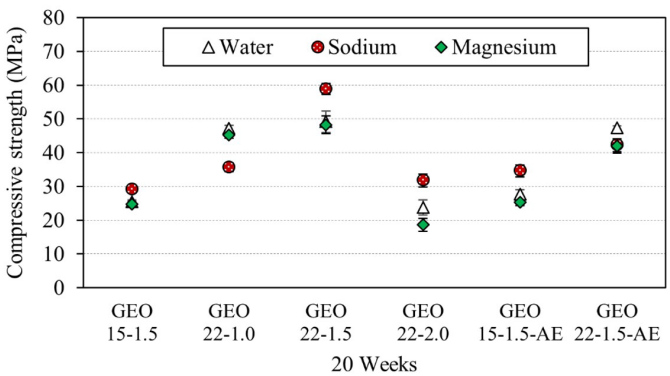

Figure 9. Mortar compressive strength results.

Table 3. Analysis of variance of mortar compressive strength after 20 weeks.

Compressive strength (MPa)							
Specimens	**Average**	***p*-value**	**Signif.**	**Specimens**	**Average**	***p*-value**	**Signif.**
GEO-15-1.5-W	25.43 ± 0.65	0.000	Sign.	GEO-22-2.0-W	23.77 ± 2.26	0.013	Sign.
GEO-15-1.5-S	29.11 ± 0.33			GEO-22-2.0-M	18.60 ± 1.93		
GEO-22-1.0-W	47.19 ± 0.83	0.000	Sign.	GEO-15-1.5-AE-W	27.73 ± 1.29	0.000	Sign.
GEO-22-1.0-S	35.65 ± 1.25			GEO-15-1.5-AE-S	34.59 ± 1.79		
GEO-22-1.5-W	49.19 ± 3.18	0.001	Sign.	GEO-22-1.5-AE-W	47.39 ± 0.60	0.002	Sign.
GEO-22-1.5-S	58.88 ± 1.66			GEO-22-1.5-AE-M	42.03 ± 2.11		
GEO-22-2.0-W	23.77 ± 2.26	0.001	Sign.				
GEO-22-2.0-S	31.79 ± 1.92						

Note: W=water, S= Na_2SO_4, M= $MgSO_4$, AE= Air-Entraining and Sign.=Significant.

In the $MgSO_4$ solution, no increase in resistance was recorded and the most important reduction of 21.7% occurred in the GEO-22-2.0-M specimens, justified by the occurrence of expansion, formation of caminite in the surface region and the M-A-S-(H). Although the expansion of the GEO-22-2.0-S specimens was greater (≈ 0.19%) than the GEO-22-2.0-M specimens (≈ 0.12%), the geopolymer structure changed with this formulation (Ms = 2.0) was more affected compared to Ms = 1.0 and 1.5. Therefore, the decrease in compressive strength of the GEO-22-2.0-M samples exposed to magnesium sulfates was mainly due to the formation of the caminite and M-A-S-(H) phases, resulting from the ion exchange process of the amorphous phase of the geopolymer when immersed in $MgSO_4$ solution as indicated in other research [28]–[30]. Furthermore, the addition of air-entraining additive did not improve the compressive strength of geopolymers during attacks by sodium and magnesium sulfates, since lower resistances are recorded compared to samples without the chemical additive.

The influence of sodium and magnesium sulfate attack on flexural tensile strength can be observed in Figure 10 and Table 4. Unlike compressive strength, all geopolymeric samples exposed to magnesium sulfates for 20 weeks showed a decrease in strength flexural tensile strength of up to 32.9% (GEO-22-1.5-M), except the GEO-22-2.0-M mortars. In the GEO-22-2.0-M samples, the lower void ratio (Figure 2b) may have contributed to the increase in the effective force area and thus increased the stress-bearing capacity. In others samples immersed in $MgSO_4$, the higher absorption rate and structural changes in the gel may be associated with reduced mechanical resistance, since the M-A-S-(H) compound is indicated as a low-resistance phase in other research [29], [30].

In the sodium sulfate solution, a reduction in tensile strength of up to 44.2% (GEO-22-1.0-S) was observed when using the Na/MK = 22% content, except for the GEO specimens GEO-22-2.0-S that showed a slight increase in resistance, although not significant. In specimens formulated with Na/MK = 15%, GEO-15-1.5-S samples showed a significant increase in tensile strength of 31.2% compared to the same mixture immersed in water, while no change occurred with the addition of an air-entraining additive. The increase in strength is attributed to the continuous hydration and crystallization of sodium sulfates within the geopolymer concrete [25].

Likewise, the air-entraining additives added to geopolymer mortars did not contribute to improving the tensile strength of the specimens subjected to attack by sodium and magnesium sulfates (Na/MK = 22%), as a decrease in the mechanical resistance of 48.1% and 34.6%, respectively, were found in this research. There was also a 15% decrease in the resistance of mortars synthesized with Na/MK = 15% and exposed to $MgSO_4$. Therefore, the hypothesis of damping tensions caused by the expansive products of sulfate attack through the voids produced by the air-entraining additive was not confirmed in this study until the age tested.

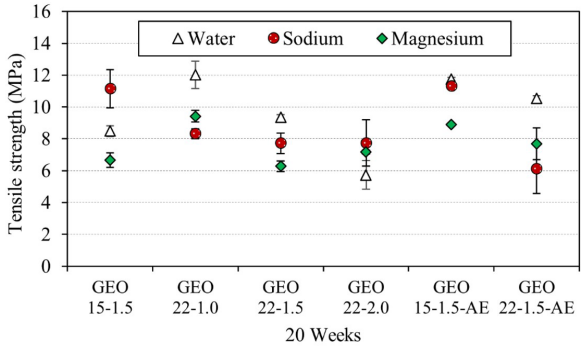

Figure 10. Results of flexural tensile strength of mortars.

Table 4. Analysis of variance of flexural tensile strength of mortars.

Flexural tensile strength (MPa)							
Specimens	**Average**	***p*-value**	**Signif.**	**Specimens**	**Average**	***p*-value**	**Signif.**
GEO-15-1.5-W	8.49 ± 0.34	0.020	Sign.	GEO-22-2.0-W	5.73 ± 0.91	0.113	NS
GEO-15-1.5-S	11.14 ± 1.20			GEO-22-2.0-S	7.74 ± 1.46		
GEO-15-1.5-W	8.49 ± 0.34	0.013	Sign.	GEO-22-2.0-W	5.73 ± 0.91	0.125	NS
GEO-15-1.5-M	6.67 ± 0.45			GEO-22-2.0-M	7.17 ± 0.13		
GEO-22-1.0-W	12.02 ± 0.86	0.011	Sign.	GEO-15-1.5-AE-W	10.56 ± 0.15	0.003	Sign.
GEO-22-1.0-S	8.33 ± 0.30			GEO-15-1.5-AE-M	8.89 ± 0.01		
GEO-22-1.0-W	12.02 ± 0.86	0.008	Sign.	GEO-22-1.5-AE-W	11.76 ± 0.11	0.015	Sign.
GEO-22-1.0-M	9.42 ± 0.37			GEO-22-1.5-AE-S	6.10 ± 1.53		
GEO-22-1.5-W	9.37 ± 0.16	0.072	NS	GEO-22-1.5-AE-W	11.76 ± 0.11	0.011	Sign.
GEO-22-1.5-S	7.73 ± 0.64			GEO-22-1.5-AE-M	7.69 ± 0.99		
GEO-22-1.5-W	9.37 ± 0.16	0.007	Sign.				
GEO-22-1.5-M	6.28 ± 0.35						

Note: W=water, S=Na_2SO_4, M=$MgSO_4$, AE=Air-Entraining, Sign.=Significant and NS=Non-Significant.

The interaction between the microstructure and sulfates resulted in fluctuations in compressive strength and flexural tensile strength. These fluctuations are due to the formation of sulfate attack products. Mixtures GEO-15-1.5, GEO-22.1.0, and GEO-22-1.5 showed compressive strengths similar to standard samples when exposed to $MgSO_4$ for 20 weeks, while in Na_2SO_4 solution, an increase in strength is recorded due to refinement temporary of pores by sulfate crystals. On the other hand, there was a decrease in flexural tensile strength in most of the specimens exposed to both sulfate solutions. Therefore, different geopolymer formulations can result in different behaviors when exposed to sodium and magnesium sulfates, although the sulfate attack products are the same regardless of the geopolymer formulation.

4 CONCLUSIONS

Based on the observation and analysis of the deterioration caused by the attack by sodium and magnesium sulfates in geopolymer mortars, the main conclusions are presented below:

- The use of a greater amount of Na_2SiO_3 in the geopolymer formulation GEO-22-2.0 (Ms = 2.0) contributes to significantly reducing the rate of water absorption by immersion. However, this samples show greater physical deterioration and expansion after immersion in sodium sulfate sodium and magnesium, compared to samples Ms = 1.0 and 1.5, attributed to leaching of the Na_2SiO_3 activator.
- The air-entraining additive used in this research did not result in significant changes in the physical appearance of the mortars after 20 weeks of exposure to sodium and magnesium sulfates, which may be associated with the insufficient time to accumulate the sulfate attack products in the air voids and cause damage to the mortars.
- The chemical elements identified in the SEM/EDS analyses were attributed to the formation of caminite and the change in the structure of the aluminosilicate gel to M-A-S-(H) in mortars exposed to $MgSO_4$, and to thenardite in mortars subjected to Na_2SO_4. However, these identifications were performed only by stoichiometry calculations and are subject to the accuracy of the technique used. The execution of other identification techniques, such as XRD, is suggested to confirm the hypotheses raised in this article.
- The mixtures GEO-15-1.5, GEO-22-1.0, and GEO-22-1.5 showed compressive strengths similar to standard samples when exposed to $MgSO_4$ for 20 weeks, while in the solution of Na_2SO_4, an increase in strength is recorded due to temporary cycles of pore refinement by sulfate crystals.
- The geopolymer formulation can result in different behaviors when exposed to sodium and magnesium sulfates, however, the products of sulfate attack are the same, regardless of the formulation used.
- This article's results are limited to the materials, dosage, and time available for the research. The influence of these parameters on sulfate attack at later ages still needs further study.

ACKNOWLEDGEMENTS

Special thanks to the Federal University of Paraná - UFPR and the Graduate Program in Civil Engineering - PPGEC, to the Paranaense University - UNIPAR, and Metacaulim do Brasil that contributed to this research being carried out. The authors also thank the Brazilian Federal Agency for the Support and Evaluation of Graduate Education (Coordenação de Aperfeiçoamento de Pessoal de Nível Superior - CAPES), the National Council for Scientific and

Technological Development (Conselho Nacional de Desenvolvimento Científico and Tecnológico - CNPQ) (process number 304474/2023-1), and the Araucária Foundation for their support in conducting this study.

5 REFERENCES

[1] N. Shehata, E. T. Sayed, and M. A. Abdelkareem, "Recent progress in environmentally friendly geopolymers: a review," *Sci. Total Environ.*, vol. 762, pp. 143166, Mar 2021, http://doi.org/10.1016/j.scitotenv.2020.143166.

[2] A. Katsiki, T. Hertel, T. Tysmans, Y. Pontikes, and H. Rahier, "Metakaolinite phosphate cementitious matrix: inorganic polymer obtained by acidic activation," *Materials*, vol. 12, no. 3, pp. 442, Jan 2019, http://doi.org/10.3390/ma12030442.

[3] S. Riahi, A. Nemati, A. R. Khodabandeh, and S. Baghshahi, "The effect of mixing molar ratios and sand particles on microstructure and mechanical properties of metakaolin-based geopolymers," *Mater. Chem. Phys.*, vol. 240, pp. 122223, Jan 2020, http://doi.org/10.1016/j.matchemphys.2019.122223.

[4] L. M. Costa, N. G. S. Almeida, M. Houmard, P. R. Cetlin, G. J. B. Silva, and M. T. P. Aguilar, "Influence of the addition of amorphous and crystalline silica on the structural properties of metakaolin-based geopolymers," *Appl. Clay Sci.*, vol. 215, pp. 106312, Dec 2021, http://doi.org/10.1016/j.clay.2021.106312.

[5] S. Pu, Z. Zhu, W. Song, W. Huo, and C. Zhang, "A eco-friendly acid fly ash geopolymer with a higher strength," *Constr. Build. Mater.*, vol. 335, pp. 127450, Jun 2022, http://doi.org/10.1016/j.conbuildmat.2022.127450.

[6] J. Yang et al., "An efficient approach for sustainable fly ash geopolymer by coupled activation of wet-milling mechanical force and calcium hydroxide," *J. Clean. Prod.*, vol. 372, pp. 133771, Oct 2022, http://doi.org/10.1016/j.jclepro.2022.133771.

[7] N. H. Jamil, M. M. A. B. Abdullah, F. Che Pa, H. Mohamad, W. M. A. Ibrahim, and J. Chaiprapa, "Influences of SiO_2, Al_2O_3, CaO and MgO in phase transformation of sintered kaolin-ground granulated blast furnace slag geopolymer," *J. Mater. Res. Technol.*, vol. 9, no. 6, pp. 14922–14932, Nov/Dec 2020, http://doi.org/10.1016/j.jmrt.2020.10.045.

[8] Y. Shi et al., "Preparation and curing method of red mud-calcium carbide slag synergistically activated fly ash-ground granulated blast furnace slag based eco-friendly geopolymer," *Cement Concr. Compos.*, vol. 139, pp. 104999, May 2023, http://doi.org/10.1016/j.cemconcomp.2023.104999.

[9] Q. An, H. Pan, Q. Zhao, and D. Wang, "Strength development and microstructure of sustainable geopolymers made from alkali-activated ground granulated blast-furnace slag, calcium carbide residue, and red mud," *Constr. Build. Mater.*, vol. 356, pp. 129279, Nov 2022, http://doi.org/10.1016/j.conbuildmat.2022.129279.

[10] A. Rossi, L. Simão, M. J. Ribeiro, D. Hotza, and R. F. P. M. Moreira, "Study of cure conditions effect on the properties of wood biomass fly ash geopolymers," *J. Mater. Res. Technol.*, vol. 9, no. 4, pp. 7518–7528, Jul/Aug 2020, http://doi.org/10.1016/j.jmrt.2020.05.047.

[11] D. Eliche-Quesada, A. Calero-Rodríguez, E. Bonet-Martínez, L. Pérez-Villarejo, and P. J. Sánchez-Soto, "Geopolymers made from metakaolin sources, partially replaced by Spanish clays and biomass bottom ash," *J. Build. Eng.*, vol. 40, pp. 102761, Aug 2021, http://doi.org/10.1016/j.jobe.2021.102761.

[12] H. E. Elyamany, A. E. M. Abd Elmoaty, and A. M. Elshaboury, "Magnesium sulfate resistance of geopolymer mortar," *Constr. Build. Mater.*, vol. 184, pp. 111–127, Sep 2018, http://doi.org/10.1016/j.conbuildmat.2018.06.212.

[13] L. Guo et al., "Sulfate resistance of hybrid fiber reinforced metakaolin geopolymer composites," *Compos., Part B Eng.*, vol. 183, pp. 107689, Feb 2020, http://doi.org/10.1016/j.compositesb.2019.107689.

[14] M. Nawaz, A. Heitor, and M. Sivakumar, "Geopolymers in construction: recent developments," *Constr. Build. Mater.*, vol. 260, pp. 120472, Nov 2020, http://doi.org/10.1016/j.conbuildmat.2020.120472.

[15] F. Pelisser, E. L. Guerrino, M. Menger, M. D. Michel, and J. A. Labrincha, "Micromechanical characterization of metakaolin-based geopolymers," *Constr. Build. Mater.*, vol. 49, pp. 547–553, Dec 2013, http://doi.org/10.1016/j.conbuildmat.2013.08.081.

[16] F. Pelisser et al., "Structural analysis of composite metakaolin-based geopolymer concrete," *Rev. IBRACON Estrut. Mater.*, vol. 11, no. 3, pp. 535–543, May 2018, http://doi.org/10.1590/s1983-41952018000300006.

[17] G. A. Ramos, F. Pelisser, P. J. P. Gleize, A. M. Bernardin, and M. D. Michel, "Effect of porcelain tile polishing residue on geopolymer cement," *J. Clean. Prod.*, vol. 191, pp. 297–303, Aug 2018, http://doi.org/10.1016/j.jclepro.2018.04.236.

[18] M. A. Longhi, Z. Zhang, B. Walkley, E. D. Rodríguez, and A. P. Kirchheim, "Strategies for control and mitigation of efflorescence in metakaolin-based geopolymers," *Cement Concr. Res.*, vol. 144, pp. 106431, Jun 2021, http://doi.org/10.1016/j.cemconres.2021.106431.

[19] Y. K. Cho, S. W. Yoo, S. H. Jung, K. M. Lee, and S. J. Kwon, "Effect of Na_2O content, SiO_2/ Na_2O molar ratio, and curing conditions on the compressive strength of FA-based geopolymer," *Constr. Build. Mater.*, vol. 145, pp. 253–260, Aug 2017, http://doi.org/10.1016/j.conbuildmat.2017.04.004.

[20] Z. Zhang, J. L. Provis, H. Wang, F. Bullen, and A. Reid, "Quantitative kinetic and structural analysis of geopolymers. Part 2. Thermodynamics of sodium silicate activation of metakaolin," *Thermochim. Acta*, vol. 565, pp. 163–171, Aug 2013, http://doi.org/10.1016/j.tca.2013.01.040.

[21] K. Chen, D. Wu, L. Xia, Q. Cai, and Z. Zhang, "Geopolymer concrete durability Subjected to aggressive environments – A review of influence factors and comparison with ordinary Portland cement," *Constr. Build. Mater.*, vol. 279, pp. 122496, Apr 2021., http://doi.org/10.1016/j.conbuildmat.2021.122496.

[22] S. Chen et al., "The influence of Si/Al ratio on sulfate durability of metakaolin-based geopolymer," *Constr. Build. Mater.*, vol. 265, pp. 120735, Dec 2020, http://doi.org/10.1016/j.conbuildmat.2020.120735.

[23] J. Obeng, A. Andrews, M. Adom-Asamoah, and S. Adjei, "Effect of calcium carbide residue on the sulphate resistance of metakaolin-based geopolymer mortars," *Clean. Mater*, vol. 7, pp. 100177, Mar 2023, http://doi.org/10.1016/j.clema.2023.100177.

[24] H. S. Arel and B. S. Thomas, "The effects of nano - and micro-particle additives on the durability and mechanical properties of mortars exposed to internal and external sulfate attacks," *Results Phys.*, vol. 7, pp. 843–851, Apr 2017, http://doi.org/10.1016/j.rinp.2017.02.009.

[25] W. Song, T. Guo, P. Han, X. Wang, F. Ma, and B. He, "Durability study and mechanism analysis of red mud-coal metakaolin geopolymer concrete under a sulfate environment," *Constr. Build. Mater.*, vol. 409, pp. 133990, Dec 2023, http://doi.org/10.1016/j.conbuildmat.2023.133990.

[26] X. Jiang, S. Mu, and J. Liu, "Influence of chlorides and salt concentration on salt crystallization damage of cement-based materials," *J. Build. Eng.*, vol. 61, pp. 105260, Dec 2022, http://doi.org/10.1016/j.jobe.2022.105260.

[27] S. Yu and C. T. Oguchi, "Is sheer thenardite attack impotent compared with cyclic conversion of thenardite–mirabilite mechanism in laboratory simulation tests," *Eng. Geol.*, vol. 152, no. 1, pp. 148–154, Jan 2013, http://doi.org/10.1016/j.enggeo.2012.10.009.

[28] C. Narattha, S. Wattanasiriwech, and D. Wattanasiriwech, "Effect of magnesium sulfate on properties of low calcium fly ash based-geopolymer- treated hemp shiv bio-concrete," *Constr. Build. Mater.*, vol. 392, pp. 131714, Aug 2023, http://doi.org/10.1016/j.conbuildmat.2023.131714.

[29] S. Jena and R. Panigrahi, "Evaluation of durability and microstructural properties of geopolymer concrete with ferrochrome slag as coarse aggregate," *Civ. Eng.*, vol. 46, no. 2, pp. 1201–1210, Jul 2022, http://doi.org/10.1007/s40996-021-00691-y.

[30] T. Long, Q. Wang, Z. Guan, Y. Chen, and X. Shi, "Deterioration and microstructural evolution of the fly ash geopolymer concrete against $MgSO_4$ solution," *Adv. Mater. Sci. Eng.*, vol. 2017, pp. 4247217, Oct 2017, http://doi.org/10.1155/2017/4247217.

[31] J. Ren, Y. Lai, J. Zhang, and W. Pei, "Whether mixed using polypropylene fiber and air-entraining agent can further improve the macro and micro durability of concrete in cold and sulfate regions," *Cold Reg. Sci. Technol.*, vol. 212, pp. 103891, May 2023, http://doi.org/10.1016/j.coldregions.2023.103891.

[32] D. M. A. Huiskes, A. Keulen, Q. L. Yu, and H. J. H. Brouwers, "Design and performance evaluation of ultra-lightweight geopolymer concrete," *Mater. Des.*, vol. 89, pp. 516–526, Jan 2016, http://doi.org/10.1016/j.matdes.2015.09.167.

[33] Y. Aygörmez, O. Canpolat, M. M. Al-mashhadani, and M. Uysal, "Elevated temperature, freezing-thawing and wetting-drying effects on polypropylene fiber reinforced metakaolin based geopolymer composites," *Constr. Build. Mater.*, vol. 235, pp. 117502, Feb 2020, http://doi.org/10.1016/j.conbuildmat.2019.117502.

[34] B. A. Tayeh, A. M. Zeyad, I. S. Agwa, and M. Amin, "Effect of elevated temperatures on mechanical properties of lightweight geopolymer concrete," *Case Stud. Constr. Mater.*, vol. 15, e00673, Dec 2021, http://doi.org/10.1016/j.cscm.2021.e00673.

[35] T. Ikumi, S. H. P. Cavalaro, I. Segura, and A. Aguado, "Alternative methodology to consider damage and expansions in external sulfate attack modeling," *Cement Concr. Res.*, vol. 63, pp. 105–116, Sep 2014, http://doi.org/10.1016/j.cemconres.2014.05.011.

[36] X. Guo and G. Xiong, "Resistance of fiber-reinforced fly ash-steel slag based geopolymer mortar to sulfate attack and drying-wetting cycles," *Constr. Build. Mater.*, vol. 269, pp. 121326, Feb 2021, http://doi.org/10.1016/j.conbuildmat.2020.121326.

[37] Associação Brasileira de Normas Técnicas, *Cimento Portland - Determinação de Variação Dimensional de Barras de Argamassa de Cimento Portland Expostas à Solução de Sulfato de Sódio*, ABNT NBR 13583, Mar., 2014.

[38] J. Zhang, C. Shi, and Z. Zhang, "Carbonation induced phase evolution in alkali-activated slag/fly ash cements: The effect of silicate modulus of activators," *Constr. Build. Mater.*, vol. 223, pp. 566–582, Oct 2019, http://doi.org/10.1016/j.conbuildmat.2019.07.024.

[39] Associação Brasileira de Normas Técnicas, *Argamassa para Assentamento e Revestimento de Paredes e Tetos – Determinação da Resistência à Tração na Flexão e à Compressão*, ABNT NBR 13279, Oct., 2005.

[40] Z. Zhang, H. Wang, J. L. Provis, F. Bullen, A. Reid, and Y. Zhu, "Quantitative kinetic and structural analysis of geopolymers. Part 1. The activation of metakaolin with sodium hydroxide," *Thermochim. Acta*, vol. 539, pp. 23–33, Jul 2012, http://doi.org/10.1016/j.tca.2012.03.021.

[41] A. M. Rashad, "Alkali-activated metakaolin: a short guide for civil engineer: an overview," *Constr. Build. Mater.*, vol. 41, pp. 751–765, Apr 2013, http://doi.org/10.1016/j.conbuildmat.2012.12.030.

[42] R. Pouhet and M. Cyr, "Carbonation in the pore solution of metakaolin-based geopolymer," *Cement Concr. Res.*, vol. 88, pp. 227–235, Oct 2016, http://doi.org/10.1016/j.cemconres.2016.05.008.

[43] M. Guerrieri, J. G. Sanjayan, and A. Z. Mohd Ali, "Geopolymer damage due to leaching when exposed to water," *Concr. Durab. Serv. Life Plann. RILEM*, vol. 26, pp. 74–78, Apr 2020, http://doi.org/10.1007/978-3-030-43332-1_15.

[44] C. Zhang et al., "Sulphate resistance of silane coupling agent reinforced metakaolin geopolymer composites," *Ceram. Int.*, vol. 48, no. 17, pp. 25254–25266, Sep 2022, http://doi.org/10.1016/j.ceramint.2022.05.190.

[45] J. W. Phair, J. S. J. van Deventer, and J. D. Smith, "Effect of Al source and alkali activation on Pb and Cu immobilisation in fly-ash based geopolymers," *Appl. Geochem.*, vol. 19, no. 3, pp. 423–434, Mar 2004, http://doi.org/10.1016/S0883-2927(03)00151-3.

[46] M. E. G. Dobrovolski, G. S. Munhoz, E. Pereira, and R. A. Medeiros-Junior, "Effect of crystalline admixture and polypropylene microfiber on the internal sulfate attack in Portland cement composites due to pyrite oxidation," *Constr. Build. Mater.*, vol. 308, pp. 125018, Nov 2021., http://doi.org/10.1016/j.conbuildmat.2021.125018.

[47] E. Pereira, E. Pereira, S. A. Pianaro, M. M. Farias, M. D. G. P. Bragança, and I. C. Oliveira, "Combined effect of alkali-aggregate reaction (AAR) and internal sulfate attack (ISA): microstructural and porous structure modifications of Portland cement mortars," *Constr. Build. Mater.*, vol. 362, pp. 129676, Jan 2023, http://doi.org/10.1016/j.conbuildmat.2022.129676.

[48] R. Luo et al., "Sulfate resistance and microstructure of metakaolin geopolymer reinforced by cellulose nanofiber and wollastonite," *J. Build. Eng.*, vol. 64, pp. 105580, Apr 2023, http://doi.org/10.1016/j.jobe.2022.105580.

Author contributions: NAMB: Conceptualization, Methodology, Formal analysis, Investigation, Writing - Original Draft; VLK: Conceptualization, Investigation, Writing - Original Draft; RS, AVT and JCNS: Investigation, Methodology; RAM: Conceptualization, Writing - Review & Editing, Supervision.

Editors: Fernando Pelisser, Daniel Cardoso.